

Upward-and-downward spread of smoldering peat fire

Xinyan Huang^{a,b,*}, Guillermo Rein^b

^a *Department of Building Services Engineering, The Hong Kong Polytechnic University, Hong Kong*

^b *Department of Mechanical Engineering, Imperial College London, UK*

Received 25 November 2017; accepted 31 May 2018

Available online 21 June 2018

Abstract

Smoldering is the dominant combustion process in peat fire, releasing a large amount of carbon and smoke into the atmosphere. The spread of smoldering in peatland is a multi-dimensional process, which is slow, low-temperature, persistent, and difficult to detect. In this work, we investigate the upward spread of peat fire from the underground to the surface after forced ignition which is a relevant configuration but rarely studied. In the experiment, ignition is not possible if the igniter is deeper than 15 cm below the free surface, regardless of moisture content or density. Once ignited, the 1st-stage upward fire spread is initiated towards the free surface (opposed smoldering) with a peak temperature of 300 °C, leaving behind a char structure that does not collapse. Then, a 2nd-stage downward spread (forward smoldering) is activated with a peak temperature of 600 °C and regression of free surface. The upward spread is faster than the downward spread. The rates of both upward and downward spread decrease as the peat density or depth is increased. These experimental observations are successfully captured by a 1D computational model of heat and mass transfer with 5-step kinetics. Modelling results further suggest that (1) the oxygen diffusion controls the entire upward-to-downward spread of peat fire, (2) the oxidation of peat sustains the 1st-stage upward spread, and (3) the oxidation of char sustains the 2nd-stage downward spread. This is the first study investigating the upward spread of peat fire, which helps understand the persistence of peat fire and guide the fire prevention and suppression strategies.

© 2018 The Author(s). Published by Elsevier Inc. on behalf of The Combustion Institute.

This is an open access article under the CC BY-NC-ND license.

(<http://creativecommons.org/licenses/by-nc-nd/4.0/>)

Keywords: Wildland fire; Opposed and forward smoldering; Critical depth; Density; Modelling

1. Introduction

Smoldering combustion is the slow, low-temperature, flameless burning of porous fuels and the most persistent type of combustion phenomena [1]. Smoldering involves heterogeneous reactions, and is sustained by the heat release when oxygen directly attacks the fuel surface [1–3],

* Corresponding author. ZS845, BLK Z, 181 Chatham Road South, Hung Hom, Kowloon, Hong Kong.

E-mail address: xy.huang@polyu.edu.hk (X. Huang).

Nomenclature

c	heat capacity [kJ/kg K]
E	activation energy [kJ/mol]
D	diffusivity [m ² /s]
h_c	heat-transfer coefficient [W/m ² K]
h_m	mass-transfer coefficient [g/m ² s]
ΔH	heat of reaction [kJ/kg]
k	thermal conductivity [W/m K]
K	permeability [m ²]
\dot{m}''	mass flux [g/m ² s]
P	Pressure [Pa]
R	universal gas constant [J/mol/K]
S	smoldering spread rate [cm/h]
t	time [s]
T	temperature [°C or K]
Y	mass fraction [–]
z	depth [cm]

Greeks

δ	thickness [m]
ν	stoichiometric coefficient [–]
ρ	density [kg/m ³]
Ψ	porosity [–]
$\dot{\omega}'''$	volumetric reaction rate [s ⁻¹ m ⁻³]

Subscripts

g	gas
i	condensed species index
j	gaseous species index
k	reaction index
s	solid

differing from high-temperature homogenous flaming combustion. It is especially common in solid fuels like coal and organic soils with a charring tendency that produce black char after the thermal decomposition. Peat, as typical organic soil, is a porous and charring natural fuel [4], thus prone to smoldering [1,5]. Smoldering fires in peatlands are the largest combustion phenomena on Earth, and annually release a huge amount of ancient carbon, roughly equivalent to 15% of man-made emissions [6,7]. Once ignited, smoldering peat fires can burn for months and years, and they destroy ecosystems and produce regional haze event all around the world. Moreover, it is difficult to detect these fires burning in depth below the ground [5].

Two mechanisms control the spread of smoldering combustion: oxygen supply and heat losses [1,3]. Most smoldering peat fires are initiated on the ground surface. After ignition, the smoldering fire can spread laterally along the free surface and vertically downward into the deep peat layers [5,8]. The dominant fire spread mode is the forward smoldering, i.e., the direction of fire spread is same as that of oxygen supply. The forward spread of smoldering peat fire has been mainly studied in the laboratory using shallow peat samples (~5 cm thick) [9–12]. Real peat fires can easily consume peat lay-

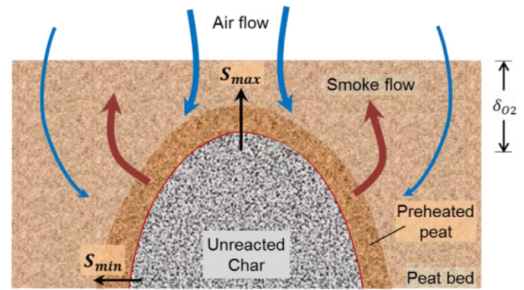


Fig. 1. Schematic diagram of multi-dimensional smoldering peat fire spreading in an upward direction.

ers of more than 50 cm [7,13], and the downward spread characteristics, as well as the depth of burn, have been investigated in [14–17]. Recent peat-fire experiments showed that the horizontal smoldering spread rate decreased with increasing moisture content (MC) [18]. However, the downward smoldering spread is controlled by the oxygen supply, and it could be faster in wetter peat if the volume of peat expands after absorbing the water [19].

Nevertheless, the peat fire can also spread upward (Fig. 1), if ignited below the free surface, e.g., self-ignition [20] or when the surface fire is suppressed while the deep fire is still alive [18]. As the oxygen from the top free surface comes in an opposed direction, the upward spread of peat fire is mostly an opposed (or reverse) smoldering. In fact, if past peat fires are not completely extinguished in the deep soil layer, when the drought season comes, these hidden fires can spread upward. Such upward fire spread is important in determining the fire risk of re-ignition and managing the fire suppression strategy. In past experiment [18], we found when the unburned peat collapsed to cover above the burning peat, it could be ignited and consumed in the form of the upward spread.

There are limited studies on the upward or opposed smoldering spread in the literature. Palmer [21] found that if ignited on the bottom, the smoldering fire can spread upward from a depth of 90 cm to free surface, and the upward spread rate was faster than in the downward model. Torero and Fernandez-Pello [22] studied the upward smoldering spread, but the smoldering fire was driven by the uprising buoyancy flow, and similar forward upward spread was conducted under forced flow [23]. Hagen et al. [24] found that the rate of upward smoldering spread increased as the fuel density decreased. He and Behrendt [25] simulated the upward and downward spread separately using the 1-step oxidation reaction and found that the upward spread is more than 10 times faster than the downward spread. They later observed a 2-stage upward-to-downward spread in experiment [26], but the mechanism behind this 2-stage spread phenomenon was not fully explored.

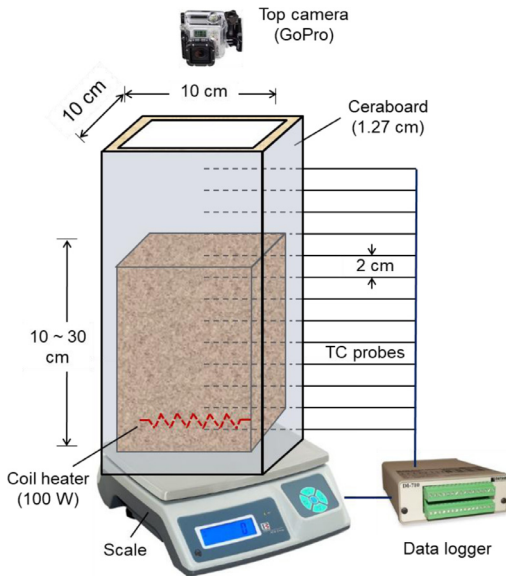


Fig. 2. Diagram of the experimental setup and the arrangement of thermocouples array.

To the best of authors' knowledge, there is no study addressing the upward spread of peat fire. In this work, we investigate the upward spread of smoldering fire in the laboratory-scale moss peat samples. The fire is initiated below the free surface, and the temperature and rate of fire spread are quantified. The numerical simulation is also conducted to reproduce the experimental phenomena and help understand the dominant chemical reactions in various stages of fire spread.

2. Experiment

2.1. Experimental setup

Figure 2 shows the schematic diagram of the experimental setup. A smoldering reactor was built using 1.27 cm thick insulation ceraboard to contain the peat sample and had an inner cross-section area of 10 cm \times 10 cm and a height of 30 cm, same as that in [19]. The reactor was further covered by several layers of aluminum foil to prevent the gas leakage and reduce the radiative heat loss. This tall peat sample was used to ensure a 1-D vertical spread mode, different from previous multi-dimensional fire spread in small and shallow peat samples [12,18].

The peat used in the experiment was typical boreal moss peat collected from an Ireland peatland. It has a mineral content $<2\%$, and has been used in several past experiments [12,18,27]. The dry peat sample was obtained by drying at 90°C for 48 h, and its bulk density is $135 \pm 5 \text{ kg/m}^3$ in its natu-

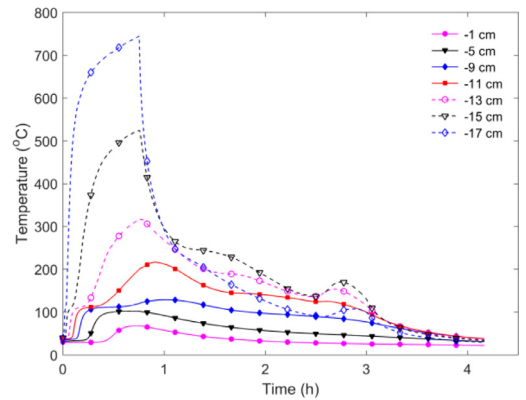


Fig. 3. Thermocouple measurements of a failed ignition in a 20-cm thick dry-peat sample after heating for 45 min. The negative sign of the thermocouple position means the distance below the initial free surface ($z=0$).

ral state. The dried peat was quickly equilibrated with the humid air to reach the MC of 5–10%. To study the effect of density, the dry peat was compressed to $190 \pm 5 \text{ kg/m}^3$. The wet peat samples of 35%, 70%, and 100% MC were also tested for ignition. In the experiment, the ambient temperature was varied between 20 and 25°C, and the ambient pressure was close to 1 atm.

To initiate an upward fire spread, a 10-cm long coil heater was placed right above the bottom insulation board. The ignition power was strong, fixed to be 100 W. The thickness of peat layer and the heating duration were adjusted to start a fire spread and find the ignition limit. A GoPro camera was hung above the sample to record the fire spread process. In addition, thermocouples (TC) probes were inserted through the sidewall into the central axis of the sample column and placed below the top free surface from 5 cm to 29 cm (near the bottom) with a 2-cm interval. These thermocouples aimed to monitor the ignition and the location of the smoldering front. The mass evolution of peat sample was measured by a scale. To ensure the repeatability, at least two experiments were conducted at each condition.

2.2. Ignitability

A successful ignition was defined if the upward fire spread was initiated and sustained. The default ignition protocol was set to 100 W for 30 min. Using the thickest dry sample (30 cm), the ignition was not successful when using the default ignition protocol. Then, the heating duration was increased to 120 min, but no ignition occurred. Ignition was still unsuccessful when the sample thickness was reduced to 20 cm, 18 cm, and 16 cm. Figure 3 shows an example of unsuccessful ignition of a 20-cm dry-peat sample after heating for 45 min.

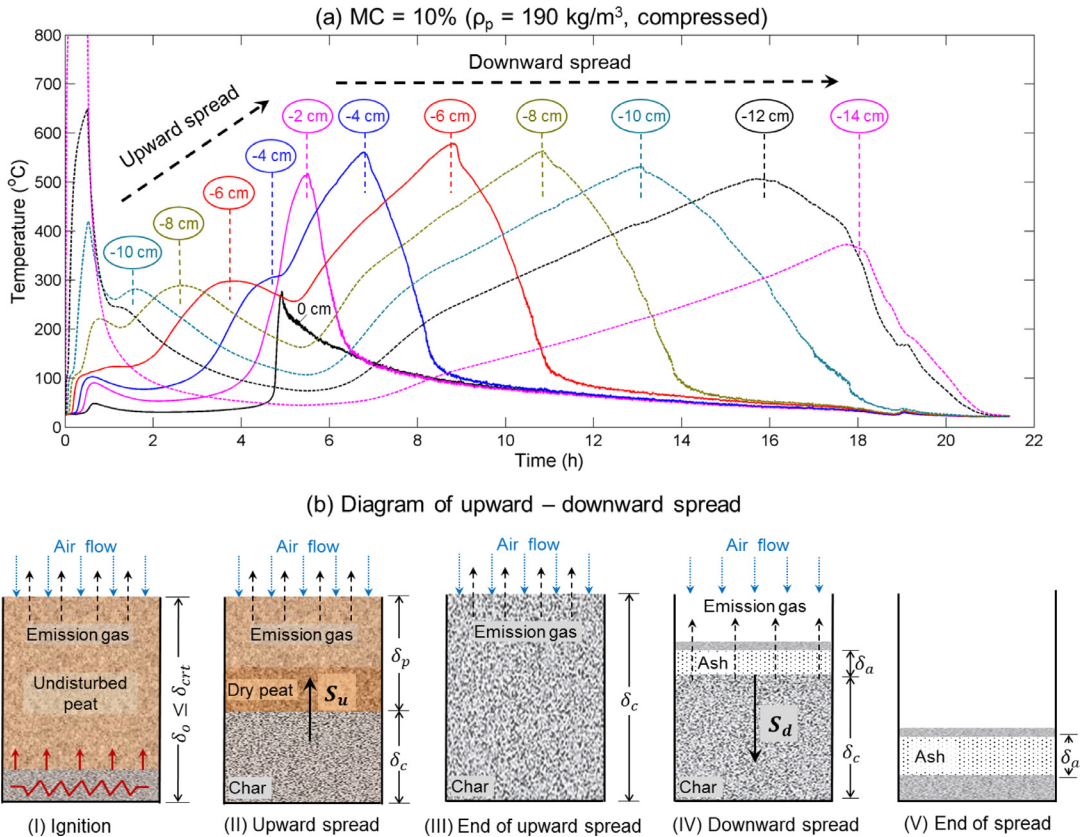


Fig. 4. (a) Thermocouple measurements in the upward fire spread over a 15-cm tall compressed peat sample with MC = 10% (dried) and $\rho_{wp} = 190 \text{ kg/m}^3$; and (b) schematic diagram of the upward spread process of smoldering peat fire. The negative sign of the thermocouple position means the distance below the initial free surface ($z = 0$).

Eventually, when a 15-cm thick sample was tested, ignition occurred under the default ignition protocol. Therefore, the critical (maximum) depth for ignition is $\delta_{max} = 15 \pm 1 \text{ cm}$. Interestingly, wet samples and compressed samples of 15-cm thickness can also be ignited under different heating durations, i.e., 30 min for 30% MC, 60 min for 70% MC, 90 min for 100% MC, and 30 min for 10% MC and 190 kg/m^3 . But no ignition occurred when the sample was thicker than 15 cm. Thus, 15 cm tends to be a universal maximum depth of ignition for this peat type, which is relatively small. Comparatively, wood sawdust (200 kg/m^3) in a depth of 90 cm [21], granular char ($365\text{--}435 \text{ kg/m}^3$) in a depth of 26 cm [26], and cotton ($5.5\text{--}100 \text{ kg/m}^3$) in a depth of 15 cm [24] can also be ignited. Thus, the fuel chemistry, porosity and permeability may have a strong effect on the maximum ignition depths. Moreover, this result also implies that the peat fire becomes difficult to sustain if it is covered by a 15-cm thick unburnt soil.

To qualitatively explain the maximum depth of ignition, we can assume there is a critical (mini-

mum) oxygen supply to achieve the ignition and sustain the upward spread. The characteristic oxygen supply under steady-state may be expressed by the Fick's law as, $\dot{m}_j = -\Psi \rho D Y_{O_2,0}/z$, which decreases as the depth (z) is increased. Thus, as the depth increases, eventually, the oxygen supply becomes too small to support the ignition.

2.3. Upward-to-downward spread

Once ignited, the peat fire started to spread upward. The video of peat fire is provided in the supplemental material. During this process, no smoke or volume change was observed. Without thermocouple readings, it was not possible to detect the existence of fire, which implies the difficulty in the detection of underground smoldering fire in peatland. Figure 4(a) shows a typical thermocouple measurement of a 15-cm thick dried (10% MC) and compressed (190 kg/m^3) peat sample ignited from the bottom (heating for 30 min). The negative sign of the thermocouple position means the distance below the free surface ($z = 0$). Figure 4(b)I-III il-

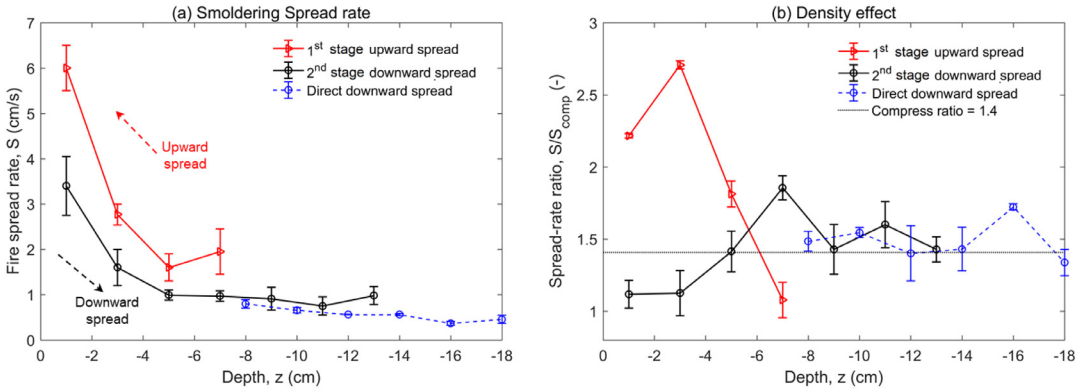


Fig. 5. (a) Rates of 1st-stage upward spread and 2nd-stage downward spread for a 15-cm thick dry and compressed peat (190 kg/m^3), compared with direct downward spread rate in [19], and (b) ratio of spread rate in normal and compressed peat. The error bars show the uncertainty of repeating tests.

illustrate the upward smoldering spread after ignition. Specifically, the upward spread lasted for 4–5 h in Fig. 4(a), and the peak temperature was relatively low (about 300°C). This low temperature suggested the existence of weak oxidation. Despite that the free surface regression was not observed, internal collapses often took place, as indicated by discontinuities in the thermocouple measurement.

When the smoldering front spread upward to near the free surface, smoke was observed. Then, a black spot appeared in the center of the top surface, and it expanded outwards until covering the entire surface. The sampling below the surface indicated that all the original peat was converted into black char during the upward spread (see Fig. 4(b)III and the video in Supplemental material). Flame was not observed in any experiment, so there is no transition from smoldering to flaming when the upward spread reached the top surface. The smoldering-to-flaming transition was observed in past upward spread experiments on polyurethane foam [22], because of different fuel chemistry and a larger oxygen supply driven by the upward buoyancy flow.

Afterwards, the smoldering front started to spread downward, as illustrated in Fig. 4(b)III and IV, and such a process was also clearly indicated by the thermocouple measurements from 5 to 22 h. During this 2nd-stage downward spread, the peak temperature was $500\text{--}600^\circ\text{C}$, much higher than the 1st-stage upward spread. Also, this temperature is similar to the direct downward spread in [19], suggesting a similar physicochemical process. Due to the heat loss from the top free surface and the bottom wall, the peak temperature decreased near these two boundaries, so the black char was not completely consumed. After extinction, a sandwich structure of fire residue (char + ash + char, see Fig. 4(b)V) was observed, which was also observed in the direct downward spread [19].

Figure 5(a) shows the measured upward and downward spread rate from Fig. 4(a), and the error bar indicates the uncertainty of repeating the experiment. Previously, a direct downward spread in the same peat sample was initiated by the ignition on the top surface [19], and its spread rate is also shown for comparison. For both the 1st-stage upward and the 2nd-stage downward spread, their spread rates decrease with the depth, same as the direct downward spread, because the oxygen supply decreases with the depth. Moreover, the upward spread was found to be much faster than the downward spread, despite a lower peak temperature, which was also observed for charcoal in [26]. There are several reasons: (1) the different dominant chemistry and transport process in the upward spread, and the combustion is not complete (discussed more with modelling in Section 3.2), and (2) the downward spread is fundamentally a “burning” like the candle [28], that is, the smoldering front only moves after the fuel is consumed. The regression of free surface also supports the burning behavior in the downward spread. On the other hand, the comparison also shows that the 2nd-stage downward spread is slightly faster than the direct downward spread, mainly because it does not have the heat sink of drying and pyrolysis that have been consumed in the 1st-stage upward spread.

Figure 5(b) shows the ratio of spread rate in normal dry peat (135 kg/m^3) to that in compressed dry peat (190 kg/m^3). Except that the spread rate near free surface (-1 cm) was relatively small because of the environmental cooling effect, in general, both upward and downward smoldering spread is faster when the peat density is smaller. It is because the rate of oxygen supply controls the rate of smoldering spread [19]. This characteristic was also observed for cotton [24]. For the downward spread, the ratio of spread rate is almost inversely proportional to the ratio of peat density (or the

compress ratio). However, for the upward spread, the effect of density on spread rate is stronger.

3. Numerical study

3.1. Model setup

To better explain the experimental results and understand the role of oxygen supply and density in both the upward and downward smoldering spread of peat fire, a 1D numerical model is applied. Previously, this model has successfully simulated the ignition process on the free surface and the consequent downward spread of peat fire. The atmospheric oxygen concentration and peat MC can be varied in the [11,19,29].

The 1-D computational domain has the same sample depth as that in the experiment, illustrated in Fig. 4(b). The details are reported in [11], only the essentials of the model are presented here: (1) condensed-phase mass conservation, (2) condensed-phase species conservation, (3) condensed-phase energy conservation, (4) gas-phase mass conservation, (5) gas-phase species conservation, and (6) gas-phase momentum conservation. All symbols are explained in the nomenclature,

$$\frac{\partial \bar{\rho}}{\partial t} = -\dot{\omega}_{fg}''' \quad (1)$$

$$\frac{\partial(\bar{\rho}Y_i)}{\partial t} = \Delta\dot{\omega}_i''' \quad (2)$$

$$\frac{\partial(\bar{\rho}\bar{h})}{\partial t} + \frac{\partial(\dot{m}''\bar{h}_g)}{\partial z} = \frac{\partial}{\partial z} \left(\bar{k} \frac{\partial T}{\partial z} \right) + \sum \dot{\omega}_{di,k}''' \Delta H_k \quad (3)$$

$$\frac{\partial(\rho_g \bar{\psi})}{\partial t} + \frac{\partial \dot{m}''}{\partial z} = \dot{\omega}_{fg}''' \quad (4)$$

$$\frac{\partial(\rho_g \bar{\psi} Y_j)}{\partial t} + \frac{\partial(\dot{m}'' Y_j)}{\partial z} = - \frac{\partial}{\partial z} \left(\rho_g \bar{\psi} D \frac{\partial Y_j}{\partial z} \right) + \Delta\dot{\omega}_j''' \quad (5)$$

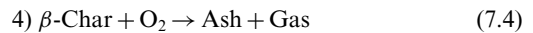
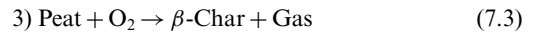
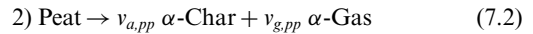
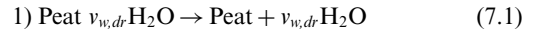
$$\dot{m}'' = - \frac{\bar{K}}{v} \frac{\partial P}{\partial z} \quad (P = \rho_g R_s T). \quad (6)$$

The model assumes the thermal equilibrium between gas and solid phase, unit Schmidt number, and the same gas diffusion coefficient and specific heat for all gas species.

At the top free surface ($z = 0$), a convection coefficient $h_c = 10 \text{ W/m}^2 \text{ K}$, capturing the environmental convective cooling, and the surface re-radiation are set. Based on the heat-mass transfer analogy, the maximum mass transfer number,

$h_m = h_c/c_p = 10 \text{ g/m}^2 \text{ s}$, is used for the gas species conservation. The ambient pressure and temperature are constant at 1 atm and 300 K, respectively. At the bottom boundary ($z = -\delta$), an external heat flux (30 kW/m^2) is applied to simulate the ignition by the coil heater, the convection coefficient is set to $5 \text{ W/m}^2 \text{ K}$, and there is no mass flux [11]. These transient equations are solved using an open-source code, Gpyro [30], and the discretization has been demonstrated in previous work [11,19].

The heterogeneous chemistry in the smoldering peat fire is described by a 5-step kinetic model, proposed previously by the thermogravimetric analysis [8,31]. The 5 steps are (1) drying (*dr*), (2) peat pyrolysis (*pp*), (3) peat oxidation (*po*), (4) β -char oxidation (βo), and (5) α -char oxidation (αo) as



where subscripts *w*, *p*, α , β , and *a* represent five condensed species: water, peat, α -char, β -char, and ash, in addition to four gaseous species: oxygen, nitrogen, water vapour, and emission gases.

The averaged properties in each cell are calculated using the appropriate mass fraction or volume fraction. The detailed species thermophysical properties and reaction kinetic parameters can be found in [19,31] (also see Supplemental material).

3.2. Numerical results

In the simulation, ignition is successful in a 15-cm thick sample, when applying a heat flux on the bottom boundary for 30 min. Figure 6 shows the simulated temperature profiles at the same location of thermocouples, in which Fig. 6(a) for the dried and compressed peat is a direct comparison to Fig. 4(a). Generally, a good agreement is also shown between simulation and experiment on (1) the duration of fire spread, and (2) the peak temperature, both of which increase with the bulk density (or the degree of compression). Most importantly, the upward-and-downward spread is successfully captured.

Figure 7 shows the simulated profile of temperature, reaction and species mass fraction duration (a) the 1st-stage upward spread, and (b) the 2nd-stage downward spread. To better compare these two stages, the moment when their peak temperatures are located at the same depth of $z = -8 \text{ cm}$ is chosen. During the upward spread, its peak

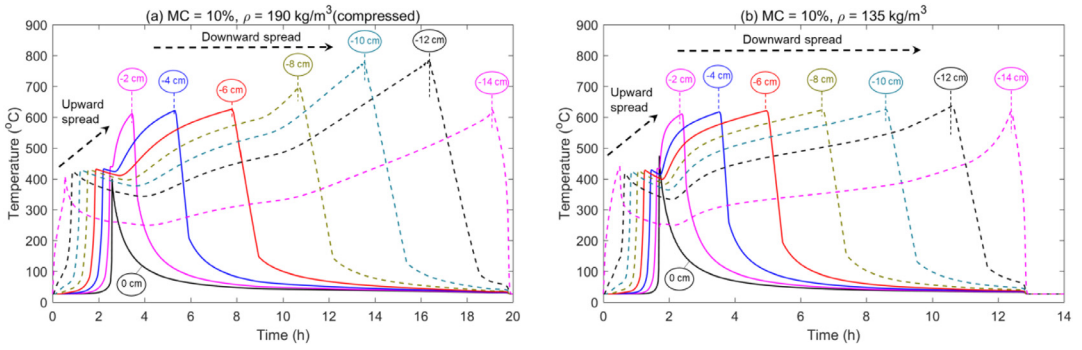


Fig. 6. Simulated temperature at different depths in the downward fire spread over a 15-cm thick dry peat sample, (a) $\rho_p = 190 \text{ kg/m}^3$ (compressed), compared with experiment in Fig. 4(a), and (b) $\rho = 135 \text{ kg/m}^3$.

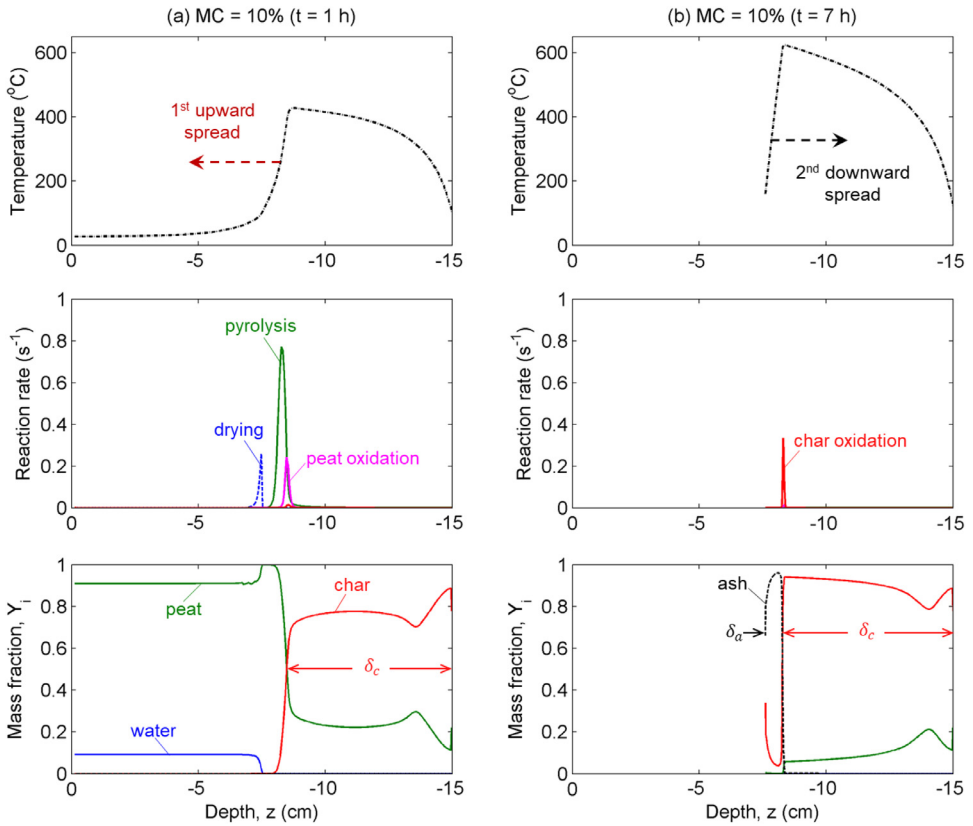


Fig. 7. Simulated profiles of temperature, reaction rate, and species mass fraction for MC = 10% (dry) and $\rho_p = 135 \text{ kg/m}^3$ at (a) $t = 1 \text{ h}$ (upward spread), and (b) $t = 7 \text{ h}$ (downward spread).

temperature is much lower than that during the downward fire spread (about 200 °C lower). Specifically, it is the low-temperature peat oxidation rather than the high-temperature char oxidation dominating the heat release to support the drying and peat pyrolysis. The combustion is not complete and even the peat is not completely oxidized, because the overall oxygen supply is small. Moreover, when

gases are released during the drying and pyrolysis, the uprising gas flow further limits the oxygen diffusion to the reaction zone.

Fundamentally, the 1st-stage upward smoldering spread is controlled by both the heat conduction and the limited oxygen supply. That is, as the peat on the top of the reaction zone is heated above the threshold temperature of peat oxidation

(< 300 °C, also see the TG data in Ref. [31]), it starts to consume oxygen, increase its temperature, and become the new reaction zone. In other words, the upward smoldering spread is the propagation of the peat-oxidation front, which is similar to the propagation of fuel-pyrolysis front in the flame spread. Meanwhile, the original reaction zone beneath is smothered and cooled under the limited oxygen supply. Also, as found in the DSC test [32], the heat release of peat oxidation is smaller than that of char oxidation, resulting in a lower peak temperature in the upward fire spread (300~400 °C). Then, during the upward spread, peat can neither be completely oxidized because of the smothering extinction nor completely pyrolyzed into char because of low peak temperature. Therefore, we predict that the upward spread rate be controlled by both the conductivity of fuel bed (proportional to density) and the rate of oxygen supply (inversely proportional to depth). After the upward fire spread, the char becomes the main composition, and the black char layer keeps growing until reaching the free surface. The growth of char agrees with the experimental observation that as the sample turned black beneath and on the free surface. Compared to the experiment in Fig. 4(a), the simulated upward spread is faster, and at a higher temperature, mainly because the model is 1-D, it does not include the heat dissipation in the horizontal direction.

The 2nd-stage downward spread is different from the 1st-stage upward spread, not only because it does not include drying and pyrolysis, but more importantly, the observed downward smoldering spread is fundamentally a burning (or fuel-consumption) process. Thus, the downward spread rate is actually the burning (or fuel-regression) rate and it is very slow. On the other hand, both the 2nd-stage downward spread and the direct downward spread initiated by the top ignition (see simulations in [19]) are slower processes and sustained at a higher temperature. Because the 2nd-stage downward spread does not contain the sub-front structures for drying and pyrolysis, it is slightly faster than the direct downward spread.

The maximum depth of ignition ($\delta_{max} = 15$ cm) is also predicted by this 1-D model when the permeability of all species is set to $K = 10^{-12}$ m². Same as the experiment, this value for maximum depth of ignition does not change with fuel density and moisture content, even if the heating duration is extended to 60 min. An unsuccessful ignition for a 20-cm dry-peat sample after heating for 45 min is shown in Fig. 8, which can be compared with Fig. 3. Although the applied heat flux cannot perfectly represent the coil heating, the trend of temperature evolution can still be well captured.

Moreover, this maximum depth is found to be sensitive to the permeability, i.e., maximum depth is larger if the permeability is larger. The real oxygen diffusion is affected by uprising flow of water

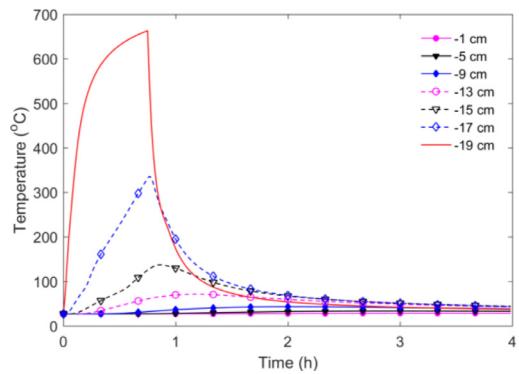


Fig. 8. Simulated temperature evolution at different depths of a failed ignition in a 20-cm thick dry-peat sample after heating for 45 min.

vapor and pyrolysis gases. Also, the overall oxygen flow is a combination of multi-dimensional diffusion and convection, which cannot be captured by this 1-D model, a future study using a 2-D model is desired. In addition, the effect of moisture is expected to affect the ease of ignition and the spread rate, which need to be further explored in future research.

4. Conclusions

In this work, we find that the forced ignition of peat is not possible, if the igniter is deeper than 15 cm below the free surface, regardless of its moisture content and density. This result implies that the smoldering fire becomes difficult to spread in peat, if it is covered by a 15-cm unburnt thick soil or reducing the oxygen supply via other suppression methods.

Once ignited, peat fire first spreads upward to the free surface in the mode of opposed smoldering with a peak temperature of about 300 °C. During this 1st-stage upward spread, the combustion (or peat consumption) is incomplete, leaving behind a char structure that does not collapse. Essentially, the upward smoldering spread is the propagation of the peat-oxidation front, which is similar to the propagation of fuel-pyrolysis front in the flame spread. Moreover, no smoke or volume change was observed, which indicates the difficulty in the detection of underground smoldering fire in peatland. Then, a 2nd-stage downward spread is activated in the mode of forward smoldering with a peak temperature of about 600 °C. Fundamentally, the 2nd-stage downward smoldering spread is a burning (or fuel-regression) process, and it is much slower than the 1st-stage upward smoldering spread. Moreover, the 2nd-stage downward spread is faster than the previously found direct downward spread which is ignited on the free surface, in other

words, the reactivity and fire hazard of peat becomes greater. It is because the heat-sink effect of drying and pyrolysis has been removed in the 1st-stage upward spread. Also, both the upward and downward spread rates decrease as the peat density or the depth is increased. Both the upward and downward spread processes are sensitive to the density and depth.

Modelling results further suggest that (1) the oxygen diffusion controls the entire upward-to-downward spread of peat fire, (2) the oxidation of peat sustains the 1st-stage upward smoldering spread, and (3) the oxidation of char sustains the 2nd-stage downward smoldering spread. This is the first study investigating the upward spread of peat fire, which helps understand the persistence of peat fire and guide the prevention and suppression strategies.

Acknowledgement

This research was funded by European Research Council (ERC) Consolidator Grant HAZE (682587). XH thanks Prof. GAO Jian (CAS Qingdao Inst of Bio-Tech) for valuable discussions.

Supplementary materials

Supplementary material associated with this article can be found, in the online version, at doi: [10.1016/j.proci.2018.05.125](https://doi.org/10.1016/j.proci.2018.05.125).

References

- [1] G. Rein, in: *SFPE Handbook of Fire Protection Engineering*, 2014, 2014, pp. 581–603.
- [2] D. Drysdale, *An Introduction to Fire Dynamics*, 3rd ed., John Wiley & Sons, Ltd, Chichester, UK, 2011.
- [3] T.J.J. Ohlemiller, *Progr. Energy Combust. Sci.* 11 (4) (1985) 277–310.
- [4] F.M. Chambers, D.W. Beilman, Z. Yu, *Mires Peat* 7 (2011) 1–10.
- [5] G. Rein, in: Claire M. Belcher (Ed.), *Fire Phenomena in the Earth System*, John Wiley & Sons, Ltd., New York, 2013, pp. 15–34.
- [6] S.E. Page, F. Siegert, J.O. Rieley, H.V. Boehm, A. Jayak, S. Limink, *Nature* 420 (50) (2002) 61–65.
- [7] U. Ballhorn, F. Siegert, M. Mason, S. Limin, S. Limin, *Proc. Natl. Acad. Sci. USA* 106 (50) (2009) 21213–21218.
- [8] X. Huang, G. Rein, *Combust. Flame* 161 (6) (2014) 1633–1644.
- [9] W.H. Frandsen, *Can. J. Forest Res.* 16 (12) (1987) 1540–1544.
- [10] W.H. Frandsen, *Can. J. Forest Res.* 27 (9) (1997) 1471–1477.
- [11] X. Huang, G. Rein, H. Chen, *Proc. Combust. Inst.* 35 (3) (2015) 2673–2681.
- [12] R.M. Hadden, G. Rein, C.M. Belcher, *Proc. Combust. Inst.* 34 (2) (2013) 2547–2553.
- [13] G. Rein, N. Cleaver, C. Ashton, P. Pironi, J.L. Torero, *Catena* 74 (3) (2008) 304–309.
- [14] B.W. Benschoter, D.K. Thompson, J.M. Waddington, et al., *Int. J. Wildland Fire* 20 (3) (2011) 418.
- [15] C. Zaccone, G. Rein, V. D’Orazio, R.M. Hadden, C.M. Belcher, T.M. Miano, *Geochim. Cosmochim. Acta* 137 (2014) 134–146.
- [16] X. Huang, G. Rein, *Int. J. Wildland Fire* 24 (6) (2015) 798–808.
- [17] J. Yang, H. Chen, N. Liu, *Energy Fuels* (2016) acs.energyfuels.6b02293.
- [18] X. Huang, F. Restuccia, M. Gramola, G. Rein, *Combust. Flame* 168 (2016) 393–402.
- [19] X. Huang, G. Rein, *Int. J. Wildland Fire* 26 (11) (2017) 907–918.
- [20] F. Restuccia, X. Huang, G. Rein, *Fire Saf. J.* 91 (2017) 828–834.
- [21] K.N. Palmer, *Combust. Flame* 1 (2) (1957) 129–154.
- [22] J.L. Torero, a.C. Fernandez-Pello, *Fire Saf. J.* 24 (1) (1995) 35–52.
- [23] L. Yermán, H. Wall, J.L. Torero, *Proc. Combust. Inst.* 36 (3) (2017) 4419–4426.
- [24] B.C. Hagen, V. Frette, G. Kleppe, B.J. Arntzen, *Fire Saf. J.* 46 (3) (2011) 73–80.
- [25] F. He, F. Behrendt, *Energy Fuels* 23 (12) (2009) 5813–5820.
- [26] F. He, F. Behrendt, *Fire Saf. J.* 46 (7) (2011) 406–413.
- [27] N. Prat-Guitart, G. Rein, R.M. Hadden, C.M. Belcher, J.M. Yearsley, *Int. J. Wildland Fire* (2016) 456–465.
- [28] X. Huang, S. Link, A. Rodriguez, S. Olson, P. Ferkul, C. Fernandez-Pello, *Proc. Combust. Inst.* 37 (2018) under review.
- [29] X. Huang, G. Rein, *Int. J. Wildland Fire* 24 (2015) 798–808.
- [30] C. Lautenberger, C. Fernandez-Pello, *Fire Saf. J.* 44 (6) (2009) 819–839.
- [31] X. Huang, G. Rein, *Bioresour. Technol.* 207 (2016) 409–421.
- [32] H. Chen, W. Zhao, N. Liu, *Energy Fuels* 25 (2) (2011) 797–803.